

Article

Characterization and Heat Transfer Assessment of CuO-Based Nanofluid Prepared through a Green Synthesis Process

Suresh Kumar Shanmugam ¹, Ajithram Arivendan ², Samy Govindan Selvamani ³,
Thangaraju Dheivasigamani ⁴, Thirumalai Kumaran Sundaresan ^{5,*} and Saood Ali ^{6,*}

¹ Faculty of Mechanical Engineering, Kalasalingam Academy of Research and Education, Srivilliputhur 626126, India; sureshme48@gmail.com

² Faculty of Mechanical Engineering, Karpaga Vinayaga College of Engineering and Technology, Chengalpattu 626126, India; ajithram867@gmail.com

³ Centre for Research in Advanced Materials and Manufacturing (RAMAM), Department of Mechanical Engineering, Academy of Maritime Education and Training, Chennai 603112, India; samygsk@gmail.com

⁴ Nano-Crystal Design and Application Lab (N-DAL), Department of Physics, PSG Institute of Technology and Applied Research, Coimbatore 641062, India; thangaraju@psgitech.ac.in

⁵ Department of Mechanical Engineering, PSG Institute of Technology and Applied Research, Coimbatore 641062, India

⁶ School of Mechanical Engineering, Yeungnam University, 280 Daehak-ro, Gyeongsan 38541, Republic of Korea

* Correspondence: thirumalaikumaran@yahoo.com (T.K.S.); saoodali@ynu.ac.kr (S.A.)

Abstract: The manufacturing of copper oxide (CuO) nanoparticles has been accomplished utilizing a green technique that relies on biologically reliable mechanisms. Aqueous solutions of copper nitrate and *Ixora Coccinea* leaf extract are used in an environmentally safe process for creating CuO nanoparticles. The characterization of the synthesized CuO nanoparticles involves the utilization of techniques such as X-ray diffractometry (XRD), scanning electron microscopy (SEM), Fourier-transform infrared spectroscopy (FTIR), and thermogravimetric analysis (TGA). CuO nanoparticles are confirmed by XRD and FTIR peak results. When the particles are measured, they range between 93.75 nm and 98.16 nm, respectively. The produced CuO nanoparticles are used to prepare the nanofluid. While conventional water exhibits a 3 °C temperature difference, nanofluid achieves a considerable temperature difference of 7 °C. As a result, it is clear that the nanofluid performs better at dispersing heat into the environment. The experiment's overall findings support the possibility of ecologically friendly, green-synthesized CuO nanoparticle-induced nanofluid as an effective heat transfer fluid that can be applied to heat transfer systems.

Keywords: green synthesis; nanoparticles; characterization; nanofluid; heat transfer



Citation: Shanmugam, S.K.; Arivendan, A.; Govindan Selvamani, S.; Dheivasigamani, T.; Sundaresan, T.K.; Ali, S. Characterization and Heat Transfer Assessment of CuO-Based Nanofluid Prepared through a Green Synthesis Process. *Ceramics* **2023**, *6*, 1926–1936. <https://doi.org/10.3390/ceramics6040119>

Academic Editor: Manuel Belmonte

Received: 11 August 2023

Revised: 15 September 2023

Accepted: 19 September 2023

Published: 22 September 2023



Copyright: © 2023 by the authors. Licensee MDPI, Basel, Switzerland. This article is an open access article distributed under the terms and conditions of the Creative Commons Attribution (CC BY) license (<https://creativecommons.org/licenses/by/4.0/>).

1. Introduction

Heat transfer is required in many applications wherever energy needs to be transferred to enhance the efficiency of the working system. The active fluid acts as a charge carrier that carries the heat from the hot section into the cold chamber. Liquid-based heat transfer systems assist combustion engines, solar collectors, power generation systems, electronics, refrigeration, air conditioning, energy storage applications, etc. [1–3]. The heat transfer capacity depends on the fluid's heat capacity at the working temperature. When heat capacity is limited, effective heat conduction needs to be improved. In such cases, adding nanomaterials plays a considerable role in enhancing heat transfer efficiency [4]. The part of the additive here is to increase the working fluid's heat capacity, thereby increasing the heat transfer. The nanomaterial possesses unique properties with a wide range of applications and has more significant advantage than a larger surface area-to-mass ratio.

A nanofluid uses nanomaterials at a lower weight percentage with a fine dispersion and lower sedimentation velocity, resulting in increased heat transfer efficiency [5,6]. Many

researchers reported increases in thermo-physical properties when using nanofluids as a working fluid for heat transfer systems [7–10]. To improve the dispersion of nanoparticles in nanofluids, instead of using a single fluid system, mixing multiple functional fluids of a desired quantity is preferred. Nanofluids with a wide variety of nanomaterials including organic nanomaterials, such as graphene, and carbon nanotubes from transition metal oxides like zinc oxides, copper oxides, titanium oxides, ferrous oxide, alumina, and silica metalloid [11–22]. Copper oxide nanoparticles are synthesized using methods such as co-precipitation, solvothermal/hydrothermal synthesis, sonochemical synthesis, sol-gel process, vapor deposition, and thermal deposition [23,24]. These synthesizing techniques, however, create toxic by-products which are harmful to the environment. Environmentally sustainable nanoparticle synthesis is vital to enhance the sustainability of all living organisms. Therefore, researchers focus on developing a system capable of preparing high-quality, more sustainable and environmentally friendly nanomaterials.

The synthesis of metal oxide nanoparticles requires the reactive agents to promote the oxidization kinetics by offering the hydrates and capping agents to regulate and promote uniform nanoparticle formation [25]. pH reagents reduce the activation energy barrier towards promoting the chemical reaction. Biological green synthesis is one of the sustainable synthesis routes to produce nanoparticles with a higher quality and lower or nullified environmental impact compared to the existing chemical synthesis techniques discussed earlier. The quality and quantity of nanoparticles produced through green synthesis depend on four key factors: the concentration of precursors, the concentration of the biological extract, the pH of the system, and the temperature of calcination/annealing for the synthesized nanoparticles [26].

Various methods of green synthesis of copper oxide nanoparticles have been discussed for decades. These methods utilize organisms (bacteria, yeast, and fungi) and plant extract. Biosynthesis based on several bacteria leads to toxicity and difficulty in incubation and isolation, leading to lower utilization of such living organisms for synthesis [27]. Plant extract, on the other hand, is a potential candidate for green synthesis due to its cost-effectiveness, excellent stability, and safe operation and handling. Plant extracts consist of biomolecules that play dual roles as both reducing and stabilizing agents during the process of copper nanoparticle synthesis [28]. Aqueous extract from *Panicum sumatrense* grains was used in experimental work on the fabrication of copper oxide (CuO) nanoparticles by Velsankar et al. [29]. Diethyl phthalate (99.18%) was identified by gas chromatography-mass spectrometry as the main active phytochemical in the grains extract. The surface Plasmon resonance band of CuO nanoparticles was detected in the UV-visible spectrum at 305 nm. A high degree of crystallinity was revealed in the X-ray diffraction pattern, and the nanoparticles' mean crystallite size was 25 nm. In order to create copper oxide nanoparticles, Zahrah Alhalili [30] used *Eucalyptus Globosus* leaf extract. The scanning electron microscopy (SEM) and dynamic light scattering (DLS) analyses reveal that the spherical copper oxide nanoparticles, synthesized using a green method, exhibit an average particle size of 88 nm and a zeta potential of -16.9 mV.

Iftikhar Hussain Shah [31] examines the anti-pathogenic properties of copper oxide nanoparticles (CuO NPs) via *Calotropis procera*-mediated production. To confirm the bio-fabrication of CuO nanoparticles mediated by *Calotropis procera*, diverse microscopic and spectroscopic characterization methods were employed. These included X-ray diffraction (XRD), Fourier-transform infrared spectroscopy (FTIR), UV-visible spectrophotometry (UV), SEM and transmission electron microscopy (TEM). According to the XRD measurements, the particles exhibited high crystallinity and spanned a size range of 40 to 100 nm. CuO NPs were produced by Selvam Sathiyavimal et al. [32] using a green chemistry approach and *Abutilon indicum* leaf extract. The CuO nanoparticles produced through biogenic means were subjected to analysis using a field emission scanning electron microscope, UV, FTIR, XRD, and energy-dispersive X-ray spectroscopy (EDAX). By employing the agar well diffusion technique, the CuO NPs were synthesized which exhibited antibacterial effective-

ness against a range of human pathogenic organisms, encompassing both Gram-negative and Gram-positive bacteria.

Ixora coccinea Linn. (Rubiaceae), commonly known as jungle geranium and red *Ixora*, is an evergreen shrub found all over India. Owing to its medicinal properties, the flowers, leaves, roots, and stem are used to treat various ailments in the Indian traditional system of medicine, the Ayurveda. Phytochemical studies indicate that the plant contains phytochemicals such as lupeol, ursolic acid, oleanolic acid, sitosterol, rutin, leucocyanadin, anthocyanins, proanthocyanidins, glycosides of kaempferol, and quercetin. Pharmacological studies suggest that the plant has antioxidant, antibacterial, gastroprotective, hepatoprotective, anti-diarrheal, antinociceptive, antimutagenic, antineoplastic, and chemopreventive effects. The *Ixora coccinea* leaves were considered because of their availability and environmentally friendly nature, which reduces the reliance on traditional chemical methods that can be harmful to the environment due to the use of toxic chemicals and by-products. The *Ixora coccinea* leaf extract can play the role of both a reducing and a stabilizing agent, which makes the process economical. The *Ixora coccinea* leaf extract was also found to be non-toxic. The pH of the leaf extract was around 6 to 6.5, and it was adjusted to 10 using 0.1 M NaOH.

Synthesis of gold nanoparticles in aqueous medium using flower extracts of *Ixora coccinea* as the reducing and stabilizing agent has been reported by [33]. Only a few reports were available on the utilization of *Ixora coccinea* leaf extract as a reducing and stabilizing agent in the synthesis of metal nanoparticles.

Detailed literature research was carried out on the environmentally friendly manufacturing of CuO nanoparticles for various uses. Creating CuO-based nanofluids for thermal heat transfer applications is still feasible using green synthesis techniques. CuO NPs are produced in this work using the plant leaves of *Ixora coccinea*, copper nitrate and sodium hydroxide solutions. The CuO NPs are characterized and a nanofluid is also created. Changes in heat transfer are seen when CuO NP-based nanofluids are employed.

2. Materials and Methods

2.1. Chemicals and Reagents

In this study, the copper precursor and extra-pure copper nitrate hexahydrate ($\text{Cu}(\text{NO}_3)_2 \cdot 6\text{H}_2\text{O}$) were acquired from United Solutions in Madurai, India. The experimental setup involved stirring the mixture while gradually introducing 25 mL of NaOH using a syringe. The solvent used was green water, and all glassware was meticulously cleaned and dried with distilled water prior to the experiments.

2.2. Preparation of CuO Nanoparticles

In the context of this study, the synthesis of CuO nanoparticles was carried out utilizing an environmentally friendly synthesis approach. Around 500 g of fresh leaves of *Ixora coccinea* were harvested and thoroughly washed with regular water. The leaf extract was prepared by grinding the leaves in a mortar and then in a mixer while gradually adding distilled water (approximately 75 mL) to assist the process of grinding. The leaf extract mixture was allowed to ferment in a covered beaker wrapped in aluminium foil for about 24 h, resulting in aspergillus-infused fermented leaf extract. About 300 mL of distilled water was added to the aspergillus-infused fermented leaf extract and mixed well to obtain the leaf mixture solution, which served as the green water for CuO synthesis. The filtration process was carried out using Whatman No.1 filter paper in three 100 mL beakers sequentially to obtain 250 mL of green water after filtering the entire 300 mL leaf extract solution. Subsequently, the green water was mixed with 10 g of copper nitrate twice to facilitate the production of copper oxide.

Upon adding copper nitrate to the green water, the mixture was kept on the magnetic stirrer for two hours at 330 rpm, until it transformed from brown water into a vivid green shade. While the solution was being stirred, a gradual introduction of 25 mL of 0.1 M NaOH was carried out using a syringe. The addition of NaOH maintains the pH and controls the

nucleation and growth of nanoparticles. The overall colour of the solution transitioned from green to blue, and the solution was subjected to magnetic agitation for a period of 24 h eventually resulting in the visible formation of nanoparticle clusters akin to powder. These particles progressively settled at the bottom of the beaker after the agitation. The liquid fraction of the solution was then carefully extracted using a syringe, leaving behind the settled particles within the beaker. The remaining composite was exposed to air and allowed to naturally desiccate throughout the night, facilitating the evaporation of a significant portion of the liquid component. Following this, the composite was subjected to a two hour thermal treatment at 80 °C to further eliminate residual liquid. Subsequently, the resultant mixture was loaded into crucibles, initiating the annealing process.

The ultimate extraction of the refined CuO nanoparticles involved subjecting the composite to an annealing procedure within a chamber heated to 400 °C. Subsequent to the annealing process, the particles were carefully retrieved from the chamber and the container. The CuO nanoparticles were produced through the green synthesis method employing *Ixora coccinea*. A yield of 3.678 g of CuO nanoparticles was achieved. A schematic depiction of the CuO nanoparticles' green synthesis utilizing *Ixora coccinea* leaves is presented in Figure 1. The particles underwent characterization through XRD, SEM, and EDAX.

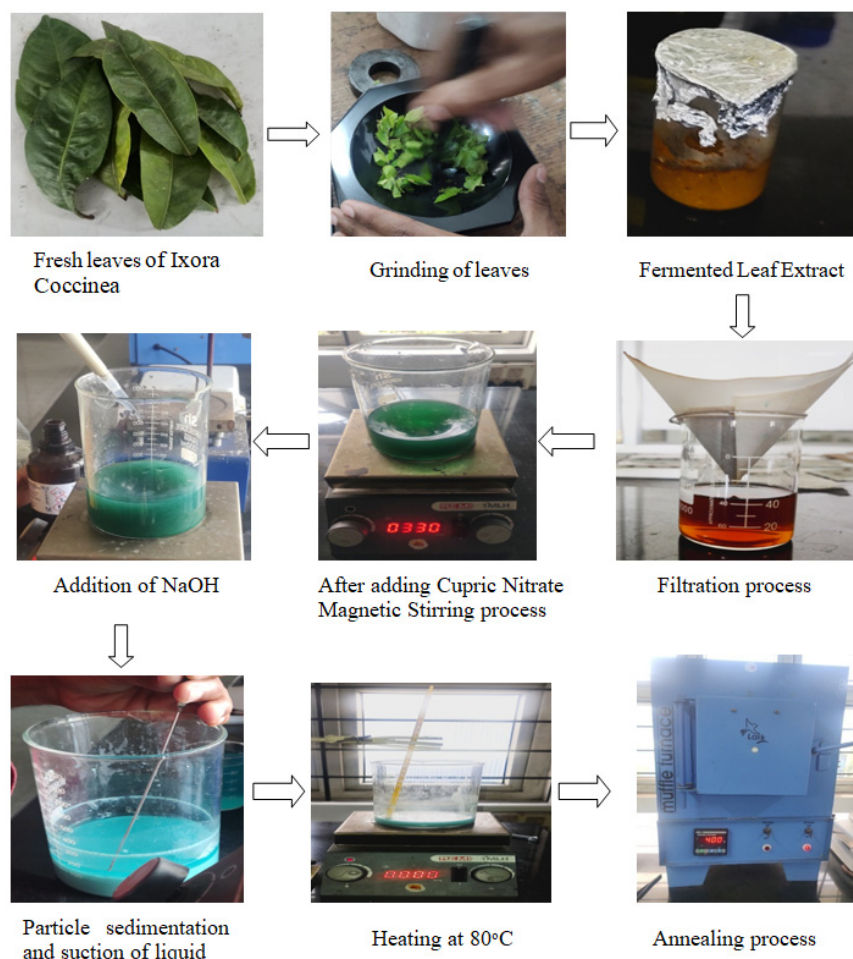


Figure 1. Process involved in the eco-friendly green synthesis of CuO nanoparticles.

2.3. Characterization Studies

For this study, XRD analysis was carried out using a D8 Advance Bruker diffractometer. The diffraction data were gathered within a range of 20° to 80° at a scanning rate of 2° /min. The resulting diffractogram was processed using the X'pert High Score Plus software version 2.1.0. The FTIR measurements were conducted on KBr pellets utilizing a Perkin Elmer Frontier MIR/FIR spectrophotometer, USA. A SEM from ZEISS, (Atlanta, GA, USA)

was employed for sample analysis. Additionally, thermogravimetric analysis (TGA) was carried out using a PerkinElmer STA 6000 thermal analyzer, USA, subjecting the samples to a temperature range of 25 °C to 750 °C.

2.4. Preparation of CuO Nanofluids

In this experiment, one gram of CuO nanoparticles was initially mixed with one litre of regular water to form the nanofluid. The magnetic stirring and ultrasonication helped to disperse the nanoparticles and prevent settling or aggregation. The magnetic stirring was performed at 300 rpm for two hours and the sonication at 1 MHz (approx.) for 30 min. The higher frequency was selected as it would be more effective for smaller nanoparticles. Finally, a total volume of 2 L of nanofluid was prepared and used for further testing and analysis.

2.5. Measurement of Heat Transfer

In the research setup, the first step involves placing a 1 L beaker filled with ordinary water onto the heating unit. Subsequently, an alcohol thermometer is introduced into the beaker to monitor the temperature of the heated fluid. The thermometer is securely mounted on the heating device platform. To gauge the input and output temperatures of the working fluid, two additional 5 L beakers are prepared and placed alongside the heating setup. Copper pipes are submerged in the hot water beaker, and these pipes are used to connect the two 5 L beakers. The connections are established using hose, pipe joints, and hose clamps. At one end of the copper pipe, a fish tank engine is attached, which will be submerged in one of the 5 L beakers while the other end remains open to the second 5 L beaker. This setup facilitates the circulation and transfer of the working fluid between the three beakers for the experimental investigation.

This experimental configuration is employed to quantify the temperature difference resulting from heat transfer interactions between the heated fluid and the working fluid at ± 0.5 °C error. Initially, ordinary water is heated and maintained at 70 °C within a 1 L beaker, serving as the hot fluid. Subsequently, a volume of 2 L of the designated working fluid is introduced into a separate 5 L beaker, maintained at room temperature (33 °C). These beakers are interconnected using copper tubes, hose pipes, and couplings, facilitating the circulation of the working fluid through the system upon submerging the motor. The activation of the motor initiates the flow of the working fluid through the copper pipe arrangement submerged in the heated fluid beaker, enabling heat absorption. An additional 5 L beaker is designated for receiving the discharged working fluid. Employing alcohol thermometers immersed at both the intake (prior to interaction with the hot fluid) and the outlet (after heat exchange) of the working fluid enables temperature measurements. The resulting temperature values are documented, enabling the determination of temperature discrepancies and the inference of heat transfer occurrences.

3. Results and Discussion

3.1. XRD Analysis

Amorphous formations typically indicate the secondary phase of thermosetting. As a result, as the reinforcement phase is combined with the sample, its structure is changed. In earlier work, the crystallinity index of samples was investigated using amorphous peak subtraction, peak height, and deconvolution techniques. The biosynthesized CuO NPs are seen in the diffractogram below. The diffraction peaks observed at positions $2\theta = 33.423$, 35.365, 38.341, and 49.652 were attributed to the Miller indices (hkl) representing the diffraction planes (110), (002), (111), and (202), respectively. Figure 2 illustrates this pattern as a hexagonal quartzite structure with pure CuO. The absence of further peaks validates the sample's high degree of purity.

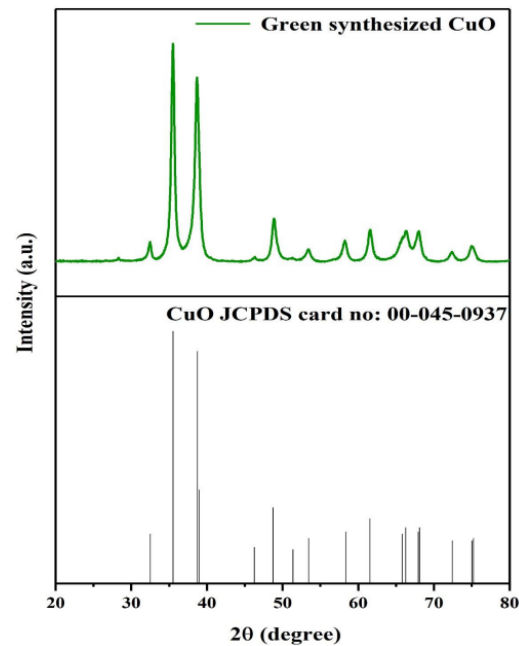


Figure 2. XRD analysis.

3.2. FTIR Analysis

The FTIR spectrum obtained from the CuO samples calcinated at 750 °C using a Shimadzu spectrometer, Japan, revealed distinct absorption bands. In Figure 3, a broad absorption band at 3368 cm^{-1} was attributed to the O-H stretching vibration of adsorbed water. The bands observed at 2917 cm^{-1} and 2274 cm^{-1} were linked to the stretching of C-H molecules. The presence of the carboxyl group was indicated by the band at 1625 cm^{-1} , which corresponds to C=O stretching. Additionally, the symmetrical and asymmetrical vibrations in the -OOH group were represented by the bands at 1395 cm^{-1} and 1407 cm^{-1} , respectively. The band at 862 cm^{-1} likely originated from C-O stretching, while the aromatic rings and their functional groups were associated with the bands at 1126 cm^{-1} and 1033 cm^{-1} .

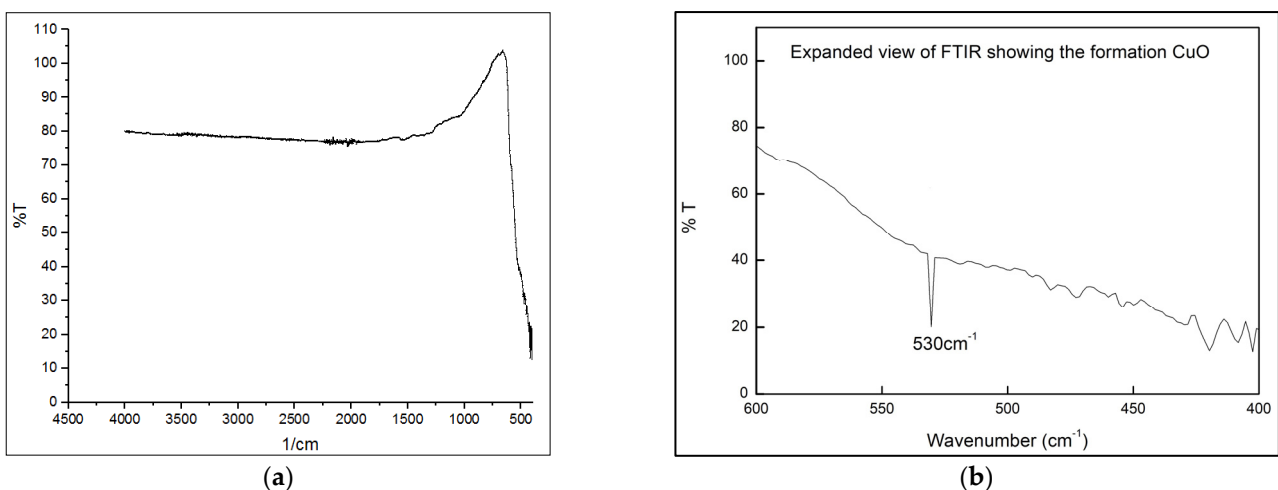


Figure 3. (a) FTIR analysis; (b) expanded view of FTIR to confirm CuO formation.

The stabilization of CuO nanoparticle crystallization was attributed to the presence of the carboxyl group in the protein. Moreover, the distinct band at 530 cm^{-1} provided confirmation of the creation of CuO particles, as it corresponded to the Cu-O stretching mode. Flavonoids and polyphenols may be prevented from clumping together by forging

a solid link with copper (Cu) during the complication process. The findings of this study agree with those of earlier ones.

3.3. Morphological Studies

Scanning electron micrographs were used to analyse the form and nature of the aggregation of the CuO NPs produced during the biosynthetic process. The morphology of the CuO NPs made from solid CuO and their agglomerated shape is shown in Figure 4. It has been proposed that the combustion processes that take place during the synthesis process may be a possible explanation for the agglomerated appearance of the chemicals. CuO NPs were produced utilizing the green technique, and the SEM results were compared to those from earlier investigations. The biosynthesized CuO nanoparticles were subjected to an EDAX examination to ascertain their composition and purity. Figure 5 displays the copper oxide EDAX spectrum and summarises its physical characteristics. The results revealed that the percentage of copper is 70.03 and that of oxygen is 11.36 in the synthesized particles. When the particles were measured, it was discovered that they ranged between 93.75 nm and 98.16 nm.

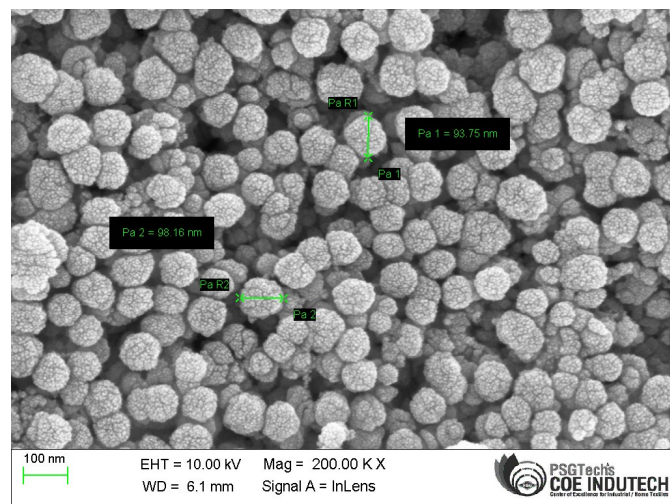


Figure 4. Microstructure.

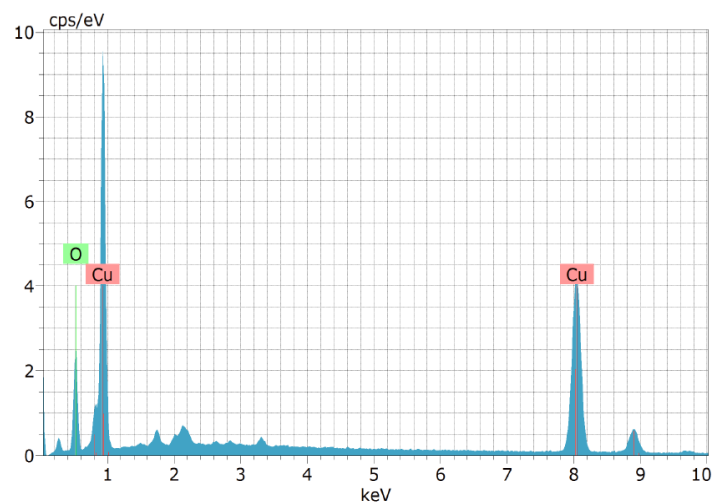


Figure 5. EDAX spectrum analysis.

3.4. Thermal Studies

The Differential Thermal Analysis (DTA)/TGA graph presented in Figure 6a,b shows the initial state of the CuO NPs prior to undergoing calcination. The temperature range

for the calcination process was set between 25 °C and 750 °C, utilizing a heating rate of 10 °C/min in a nitrogen atmosphere.

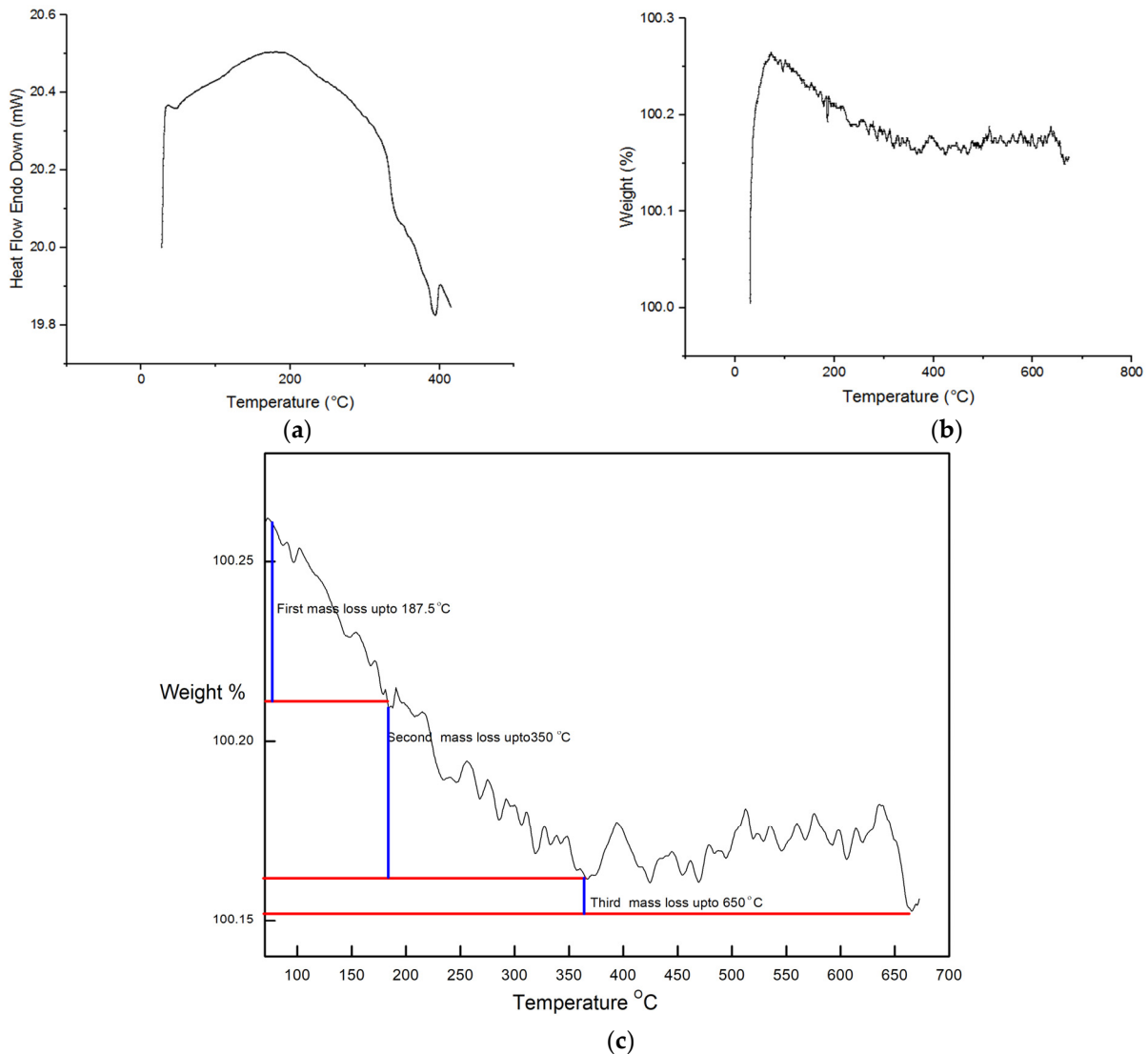


Figure 6. (a) DTA analysis, (b) TGA analysis, and (c) expanded view of TGA.

The TGA analysis conducted on the CuO revealed distinctive steps of mass loss. The initial mass loss step, accounting for 1.39% of the total mass, was observed before reaching 187.5 °C. This preliminary loss in mass can be attributed to the process of dehydration that occurs during this phase. The second mass loss happened due to the elimination of chemisorbed hydroxyl groups during the heating process between 187.5 °C and 350 °C. The oxidation of leftover organic components at temperatures between 350 °C and 512 °C was the third and last phase in the process (0.4%). No further mass was lost after 512.5 °C until 750 °C.

3.5. Heat Transfer Studies

Using the heat transfer device depicted in Figure 7, the ability of the produced NP-based nanofluid to transfer heat is evaluated. The experiment was conducted using (i) hot water as the hot fluid and regular water as the working fluid; and (ii) hot water as the hot fluid and a nanofluid as the working fluid. Following the experimental study, it is understood that a 3 °C temperature difference can be deduced when using ordinary water as the working fluid. A 7 °C difference is found while a nanofluid is employed as the

working fluid. Therefore, it makes sense that the nanofluid performs better at dispersing heat to the environment and conducting it. Compared to ordinary water, it is employed in heat transfer applications, and it is claimed that the nanofluid has the desirable thermal characteristics needed to function well as a heat exchanger. The experimental findings are shown in Table 1.

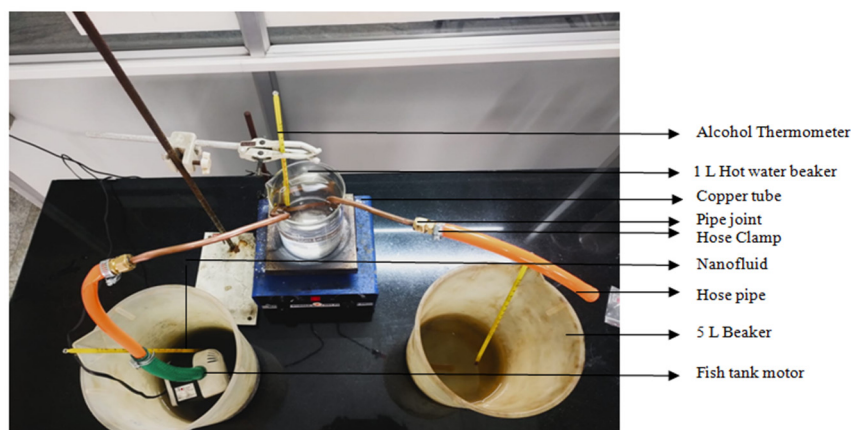


Figure 7. Heat transfer apparatus.

Table 1. Experimental results.

| Working Fluid | Inlet Temperature (°C) | Outlet Temperature (°C) | Hot Fluid Temperature (°C) | Temperature Difference (°C) |
|---------------|------------------------|-------------------------|----------------------------|-----------------------------|
| Normal Water | 33 | 36 | 70 | 3 |
| Nanofluid | 33 | 40 | 70 | 7 |

4. Conclusions

This study examines how well CuO nanoparticles made via green synthesis transfer heat and considers how they may be utilized to increase thermal conductivity. Below are some key findings from this experimental effort.

- The effective implementation of plant extracts as both reducing and stabilizing agents in the production of CuO NPs provides compelling evidence for the success of green synthesis methodologies. This approach aligns with sustainability guidelines and decreases the harmful environmental effects of nanoparticle production.
- XRD, SEM, and EDAX analyses validated the findings that the generated CuO NPs showed the desired structural and morphological features. When the particles were measured, it was discovered that they ranged between 93.75 nm and 98.16 nm.
- The fluids that had been infused with nanoparticles demonstrated good stability and dispersion, demonstrating that the CuO nanoparticles had been effectively absorbed and suspended within the base fluids. This property makes it possible to consistently and effectively improve heat transfer, which is essential for real-world applications.
- It is understood that a 3°C temperature difference can be deduced when using ordinary water as the working fluid. A 7 °C difference is found while nanofluid is employed as the working fluid.
- The increase in thermal conductivity with the rise in nanoparticle concentration implies that it is possible to finely tune heat transfer performance by adjusting the loading of nanoparticles.

The experiment's overall findings support the possibility of ecologically friendly, green-synthesized CuO nanoparticle-induced nanofluid as an effective heat-transfer fluid that can be applied to heat-transfer systems.

Author Contributions: Conceptualization, T.K.S. and S.K.S.; methodology, S.G.S.; investigation, T.K.S.; resources, T.K.S.; data curation, T.D. and A.A.; writing—original draft preparation, S.K.S.; writing—review and editing, S.A. and S.G.S.; visualization, A.A.; supervision, S.A. and T.K.S.; project administration, T.D. and T.K.S. All authors have read and agreed to the published version of the manuscript.

Funding: This research received no external funding.

Institutional Review Board Statement: Not applicable.

Informed Consent Statement: Not applicable.

Data Availability Statement: The authors confirm that the data supporting the findings of this study are available within the article.

Conflicts of Interest: The authors declare no conflict of interest.

References

1. Ganvir, R.B.; Walke, P.V.; Kriplani, V.M. Heat transfer characteristics in nanofluid—A review. *Renew. Sustain. Energy Rev.* **2016**, *75*, 451–460. [[CrossRef](#)]
2. Garcia, E.J.; Bahamon, D.; Vega, L.F. Systematic search of suitable metal–organic frameworks for thermal energy-storage applications with low global warming potential refrigerants. *ACS Sustain. Chem. Eng.* **2021**, *9*, 3157–3171. [[CrossRef](#)]
3. Elsayed, A.; Elsayed, E.; Al-Dadah, R.; Mahmoud, S.; Elshaer, A.; Kaialy, W. Thermal energy storage using metal–organic framework materials. *Appl. Energy* **2017**, *186*, 509–519. [[CrossRef](#)]
4. Choi, S.U.S.; Eastman, J.A. Enhancing thermal conductivity of fluids with nanoparticles. In *Developments and Applications of Non-Newtonian Flows*; Singer, D.A., Wang, H.P., Eds.; American Society of Mechanical Engineers: New York, NY, USA, 1995; pp. 99–105.
5. Colangelo, G.; Diamante, N.F.; Milanese, M.; Starace, G.; de Risi, A. A Critical Review of Experimental Investigations about Convective Heat Transfer Characteristics of Nanofluids under Turbulent and Laminar Regimes with a Focus on the Experimental Setup. *Energies* **2021**, *14*, 6004. [[CrossRef](#)]
6. Sajid, M.U.; Ali, H.M. Recent advances in application of nanofluids in heat transfer devices: A critical review. *Renew. Sustain. Energy Rev.* **2019**, *103*, 556–592. [[CrossRef](#)]
7. Heris, S.Z.; Shokrgozar, M.; Poorpharhang, S.; Shanbedi, M.; Noie, S.H. Experimental Study of Heat Transfer of a Car Radiator with CuO/Ethylene Glycol-Water as a Coolant. *J. Dispers. Sci. Technol.* **2014**, *35*, 677–684. [[CrossRef](#)]
8. Colangelo, G.; Favale, E.; Milanese, M.; de Risi, A.; Laforgia, D. Cooling of electronic devices: Nanofluids contribution. *Appl. Therm. Eng.* **2017**, *127*, 421–435. [[CrossRef](#)]
9. Sarafraz, M.M.; Tian, Z.; Safaei, M.R.; Goodarzi, M. Nano-Suspension in a Compact Heat Exchanger. *Energies* **2019**, *12*, 17.
10. Hu, J.; Liu, C.; Li, Q.; Shi, X. Molecular simulation of thermal energy storage of mixed CO₂/IRMOF-1 nanoparticle nanofluid. *Int. J. Heat Mass Transf.* **2018**, *125*, 1345–1348. [[CrossRef](#)]
11. Mert, S.; Yeter, A.; Yasar, H.; Topuz, A.; Durmaz, U.; Engin, T. An experimental study on cooling performance of a car radiator using Al₂O₃-ethylene glycol/water nanofluid. *Therm. Sci.* **2021**, *25*, 801–809. [[CrossRef](#)]
12. Satti, J.R.; Das, D.K.; Ray, D.R. Measurements of Densities of Propylene Glycol-Based Nanofluids and Comparison with Theory. *J. Therm. Sci. Eng. Appl.* **2016**, *8*, 021021. [[CrossRef](#)]
13. Topuz, A.; Engin, T.; AlperÖzalp, A.; Erdögan, B.; Mert, S.; Yeter, A. Experimental Investigation of Optimum Thermal Performance and Pressure Drop of Water-Based Al₂O₃, TiO₂ and ZnO Nanofluids Flowing inside a Circular Microchannel. *J. Therm. Anal. Calorim.* **2018**, *131*, 2843–2863. [[CrossRef](#)]
14. Li, H.; Wang, L.; He, Y.; Hu, Y.; Zhu, J.; Jiang, B. Experimental Investigation of Thermal Conductivity and Viscosity of EthyleneGlycol Based ZnO Nanofluids. *Appl. Therm. Eng.* **2014**, *88*, 363–368. [[CrossRef](#)]
15. Gan, Y.Y.; Ong, H.C.; Ling, T.C.; Zulkifli, N.W.M.; Wang, C.T.; Yang, Y.C. Thermal Conductivity Optimization and Entropy Generation Analysis of Titanium Dioxide Nanofluid in Evacuated Tube Solar Collector. *Appl. Therm. Eng.* **2018**, *145*, 155–164. [[CrossRef](#)]
16. Hemmat Esfe, M.; Esfandeh, S. Rheological Behavior of CuO/EG:W (20:80 v/v) Nanofluid from a Thermal Perspective. *J. Therm. Anal. Calorim.* **2019**, *135*, 61–72. [[CrossRef](#)]
17. Sundar, L.S.; Singh, M.K.; Sousa, A.C.M. Thermal Conductivity of Ethylene Glycol and Water Mixture Based Fe₃O₄ Nanofluid. *Int. Commun. Heat Mass Transf.* **2013**, *49*, 17–24. [[CrossRef](#)]
18. Syam Sundar, L.; Venkata Ramana, E.; Singh, M.K.; De Sousa, A.C.M. Viscosity of Low Volume Concentrations of Magnetic Fe₃O₄ Nanoparticles Dispersed in Ethylene Glycol and Water Mixture. *Chem. Phys. Lett.* **2012**, *554*, 236–242. [[CrossRef](#)]
19. Esfahani, M.A.; Toghraie, D. Experimental Investigation for Developing a New Model for the Thermal Conductivity of Silica/Water-Ethylene Glycol (40–60%) Nanofluid at Different Temperatures and Solid Volume Fractions. *J. Mol. Liq.* **2017**, *232*, 105–112. [[CrossRef](#)]

20. Selvaraj, V.; Krishnan, H. Synthesis of Graphene Encased Alumina and Its Application as Nanofluid for Cooling of Heat-Generating Electronic Devices. *Powder Technol.* **2020**, *363*, 665–675. [[CrossRef](#)]
21. Nawaz, S.; Babar, H.; Ali, H.M.; Sajid, M.U.; Janjua, M.M.; Said, Z.; Tiwari, A.K.; Syam Sundar, L.; Li, C. Oriented Square Shaped Pin-Fin Heat Sink: Performance Evaluation Employing Mixture Based on Ethylene Glycol/Water Graphene Oxide Nanofluid. *Appl. Therm. Eng.* **2022**, *206*, 118085. [[CrossRef](#)]
22. Shahsavani, E.; Afrand, M.; Kalbasi, R. Experimental Study on Rheological Behavior of Water–Ethylene Glycol Mixture in the Presence of Functionalized Multi-Walled Carbon Nanotubes: A Novel Correlation for the Non-Newtonian Nanofluid. *J. Therm. Anal. Calorim.* **2018**, *131*, 1177–1185. [[CrossRef](#)]
23. Ferrão, P.; Al, K.; Awad, S. Synthesis of ZnONanopowders by Using Sol-Gel and Studying Their Structural and Electrical Properties at Different Temperature. *Energy Procedia* **2017**, *119*, 565–570.
24. El Faham, M.M.; Mostafa, A.M.; Mwafy, E.A. The Effect of Reaction Temperature on Structural, Optical and Electrical Properties of Tunable ZnO Nanoparticles Synthesized by Hydrothermal Method. *J. Phys. Chem. Solids* **2021**, *154*, 110089. [[CrossRef](#)]
25. Pauzi, N.; Zain, N.M.; Yusof, N.A.A. Gum Arabic as Natural Stabilizing Agent in Green Synthesis of ZnO Nanofluids for Antibacterial Application. *J. Environ. Chem. Eng.* **2020**, *8*, 103331. [[CrossRef](#)]
26. Doan Thi, T.U.; Nguyen, T.T.; Thi, Y.D.; Ta Thi, K.H.; Phan, B.T.; Pham, K.N. Green Synthesis of ZnO Nanoparticles Using Orange Fruit Peel Extract for Antibacterial Activities. *RSC Adv.* **2020**, *10*, 23899–23907. [[CrossRef](#)] [[PubMed](#)]
27. Singh, D.; Jain, D.; Rajpurohit, D.; Jat, G.; Kushwaha, H.S.; Singh, A.; Mohanty, S.R.; Al-Sadoon, M.K.; Zaman, W.; Upadhyay, S.K. Bacteria assisted green synthesis of copper oxide nanoparticles and their potential applications as antimicrobial agents and plant growth stimulants. *Front. Chem.* **2023**, *11*, 1154128. [[CrossRef](#)]
28. Derakhshani, E.; Asri, M.; Naghizadeh, A. Plant-Based Green Synthesis of Copper Oxide Nanoparticles Using Berberis vulgaris Leaf Extract: An Update on Their Applications in Antibacterial Activity. *BioNanoScience* **2023**, *13*, 212–218. [[CrossRef](#)]
29. Velsankar, K.; Parvathy, G.; Mohandoss, S. Green synthesis and characterization of CuO nanoparticles using Panicum sumatrense grains extract for biological applications. *Appl. Nanosci.* **2022**, *12*, 1993–2021. [[CrossRef](#)]
30. Alhalili, Z. Green synthesis of copper oxide nanoparticles CuO NPs from Eucalyptus Globoulus leaf extract: Adsorption and design of experiments. *Arab. J. Chem.* **2022**, *15*, 103739. [[CrossRef](#)]
31. Shah, I.H.; Ashraf, M.; Sabir, I.A.; Manzoor, M.A.; Malik, M.S.; Gulzar, S.; Ashraf, F.; Iqbal, J.; Niu, Q.; Zhang, Y. Green synthesis and Characterization of Copper oxide nanoparticles using Calotropis procera leaf extract and their different biological potentials. *J. Mol. Struct.* **2022**, *1259*, 132696. [[CrossRef](#)]
32. Sathiyavimal, S.; Durán-Lara, E.F.; Vasantharaj, S.; Saravanan, M.; Sabour, A.; Alshiekheid, M.; Thuy Lan Chi, N.; Brindhadevi, K.; Pugazhendhi, A. Green synthesis of copper oxide nanoparticles using Abutilon indicum leaves extract and their evaluation of antibacterial, anticancer in human A549 lung and MDA-MB-231 breast cancer cells. *Food Chem. Toxicol.* **2022**, *168*, 113330. [[CrossRef](#)] [[PubMed](#)]
33. Baliga, M.S.; Kurian, P.J. *Ixora coccinea* Linn.: Traditional Uses, Phytochemistry and Pharmacology. *Chin. J. Integr. Med.* **2012**, *18*, 72–79. [[CrossRef](#)] [[PubMed](#)]

Disclaimer/Publisher’s Note: The statements, opinions and data contained in all publications are solely those of the individual author(s) and contributor(s) and not of MDPI and/or the editor(s). MDPI and/or the editor(s) disclaim responsibility for any injury to people or property resulting from any ideas, methods, instructions or products referred to in the content.